ACS OMEGA

http://pubs.acs.org/journal/acsodf

Article

Improved Magnetite Nanoparticle Immobilization on a Carbon Felt Cathode in the Heterogeneous Electro-Fenton Degradation of Aspirin in Wastewater

Charles Muzenda and Omotayo A. Arotiba*

Cite This: *ACS Omega* 2022, 7, 19261−19269

Read Online

ACCESS | Metrics & More | Article Recommendations | Supporting Information

ABSTRACT: Toward the improvement of the application of heterogeneous electro-Fenton in water treatment, we report a new strategy of enhancing the immobilization of a magnetite nanoparticle catalyst on a carbon felt cathode. Exploiting the intrinsic ferrimagnetic properties of magnetite nanoparticles, magnet bars were used to attach the magnetite into the void spaces of the porous carbon felt (CF) cathode. The magnetite nanoparticles were prepared by coprecipitation with variations in the molar ratios of Fe^{2+}/Fe^{3+}. The magnetite was characterized, attached onto the CF electrode with magnetic bars, and used in the heterogeneous electro-Fenton (EF) degradation of aspirin. The effects of the following on the degradation were studied: Fe^{2+}/Fe^{3+}, pH, catalyst loading concentration, and voltage. The heterogeneous EF degradation of aspirin in wastewater improved by 23% when magnetic bars were used to enhance the immobilization of the magnetite catalysts. The 1:4 Fe^{2+}/Fe^{3+} ratio resulted in the highest hetero-EF catalytic degradation of aspirin with complete degradation (100%) achieved after 140 min. For a mixture of pharmaceuticals, degradation percentages of 94.3% (aspirin), 88% (ciprofloxacin), and 80% (paracetamol) in 3 h were obtained. The magnetized magnetite on the cathode was reusable for 10 cycles. Thus, the use of magnets shows a promising strategy to avoid the leaching of ferrimagnetic nanoparticle catalysts embedded in the cathode for heterogeneous EF processes.

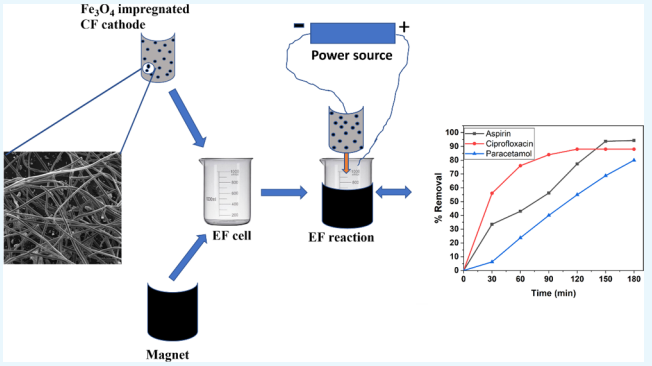

1. INTRODUCTION

Electro-Fenton (EF) oxidation of persistent organic pollutants (POPs) in water has gained much attention as an emerging electrochemical advanced oxidation process due to its advantages such as cost effectiveness, environmental friendliness, use of simple materials, and higher effectiveness in POP removal. Like all other advanced oxidation processes (AOPs), EF oxidation relies on the production of hydroxyl radicals, which in turn attack and oxidize organic contaminants in water via a chain radical reaction. The hydroxyl radical is very strong oxidant species (only second to fluorine in oxidation potential (E^0 = 2.73 V)),[1] which indiscriminately attacks organics in wastewater with the potential for complete degradation or mineralization to H_2O, CO_2, and inorganic ions.

Heterogeneous EF has gained preferential attention over homogeneous electro-Fenton reaction based on the following reasons: First, research has shown that heterogeneous EF can occur at a wider pH range than homogeneous EF, which operates within a narrow pH between 2.5 and 3.0 depending on the nature of the analyte degraded.[1,2] A wider pH application makes heterogeneous EF applicable in wider industrial applications where the polluted water can have a large variation in pH and where pH adjustment is not practicable. Second, catalyst recyclization and reusability are possible in heterogeneous EF, reducing catalyst costs.[3,4] Third, there is no accumulation of iron sludge, formed in homogeneous EF, which results in the depletion of the catalyst, thereby robbing the system of its oxidative potential toward unwanted pollutants.[2] The formation of iron sludge poses the challenge of disposal, environmental safety, and cost.[1,5,6]

Pharmaceutical wastes are among the emerging environmental contaminants that pose health risks to humans due to their toxicity and recalcitrant nature to treatment especially by traditional water treatment methods. Thus, quests for successful mitigation processes to achieve the complete remediation of this emerging class of pollutants from the environment and water have resorted to AOPs of which EF is a subset.[7−14] EF has recently been applied in the removal of

Received: January 31, 2022
Accepted: April 18, 2022
Published: June 3, 2022

Scheme 1. Heterogeneous Electro-Fenton (HEF) Setup for Magnet-Enhanced Immobilization of Magnetite Nanoparticles on the Carbon Felt (CF) Cathode

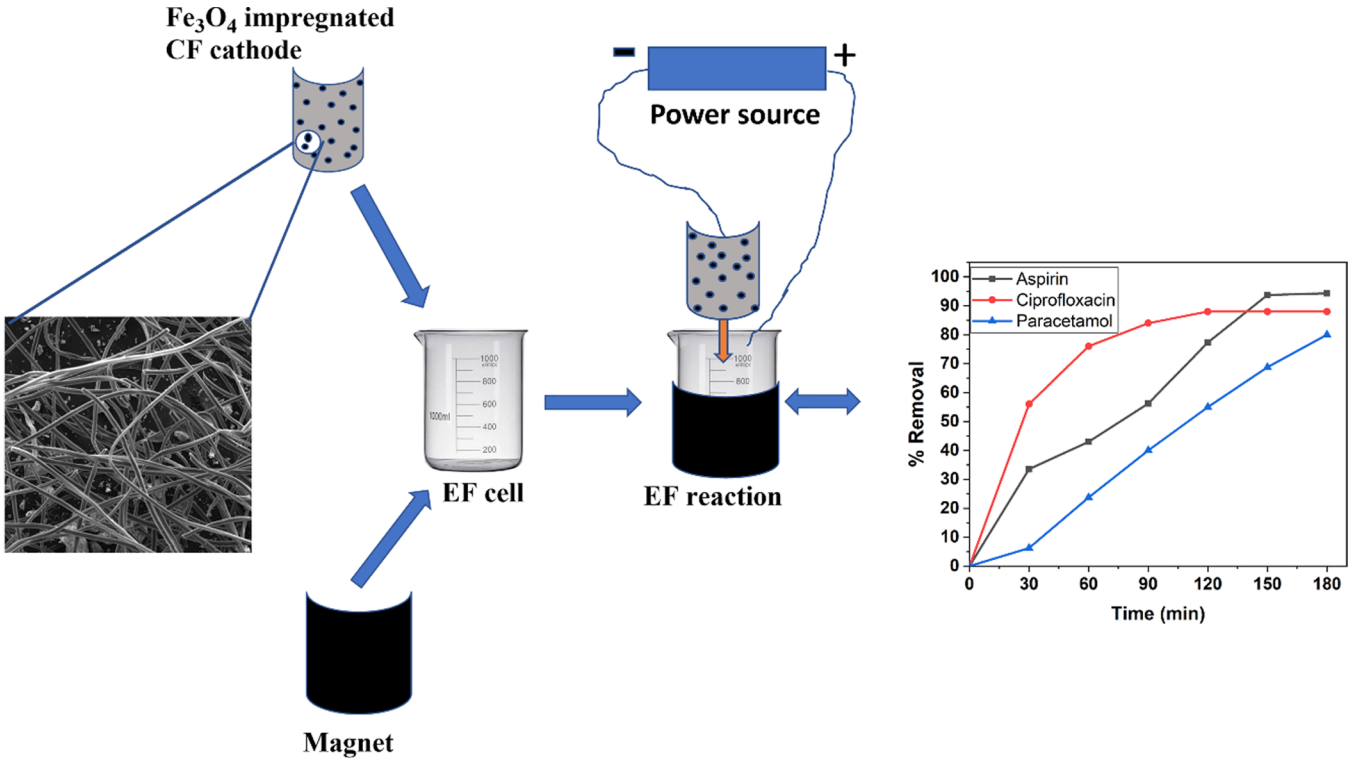

various pharmaceuticals and bacteria in effluent water in Colombia by Martínez and co-authors.[15] More similar work in the degradation of pharmaceuticals in wastewater was reported by Emeji and colleagues[16] in the removal of antiretroviral drugs, while Wang and co-authors used EF in separate work for the removal of ciprofloxacin and an antibiotic (cefoperazone), respectively.[17,18]

The advantages of heterogeneous EF have motivated research into various ways to improve the process. Some areas of interest include enhancing the production of hydrogen peroxide or hydroxyl radicals,[19,20] coupling of EF with other methods,[21,22] the type of iron source (nanoparticles),[23,24] catalyst loading, and the type of electrode used.[25−28] Toward enhancing hydrogen peroxide production, the use of electrocatalysts such as fluorine-modified carbon nanotubes for the electrochemical reduction oxygen has been reported.[21] Choice of electrodes, especially the cathode, is of interest because it can be used as a support for the iron catalyst. If the iron catalyst is in the nanoparticle form, its immobilization on the cathode can have a dual effect in that it averts the aggregation or agglomeration of the nanoparticles by acting as a support or stabilizer for even distribution. In addition to this, the cathode support can function as a redox center where reduction and regeneration of the catalyst occur.[3,29−31] The use of the cathode for catalyst immobilization thus demands careful optimization to maximize the interaction of the nanoparticles with the cathodic template without compromising the conductivity, porosity, and stability of the cathode. Equally important in the bid to improve heterogeneous EF is the recent investigations into the use of transition metal sulfide cocatalysts, taking advantage of the unstable metal sulfide bond, which readily releases the metal cations in solution for cocatalysis.[32,33]

One major challenge in the use of cathodes as the support for catalyst loading or immobilization is the leaching of the catalyst into the solution.[1,23,34−36] Leaching reduces the amount of catalyst available for the Fenton reaction and drives the process toward homogeneous EF,[37,38] which comes with the challenges highlighted earlier. There is also the possibility of passivation of the catalyst active site, and this reduces the catalytic efficiency of the nanoparticle. To sustain heterogeneous EF reaction, the problem of leaching should be mitigated by improving the interaction between the nanoparticle catalyst and the cathode material. Improved immobilization of the nanoparticle catalyst on the cathode is vital since the reaction progress heavily depends on efficient contact of the generated H_2O_2 with the catalyst for the surface reduction of ferric ions to ferrous ions (the needed EF active form). The cycle continues since ferrous ions are oxidized back to ferric ions by the Fenton reaction. The versatility of the interconversion between the Fe^{2+}/Fe^{3+} couple at all times plays a significant role in ensuring the optimal "equilibrium" concentrations of these ions to favor the production of hydroxyl radicals.

In this work, we investigated a novel approach to enhance the immobilization of magnetite nanoparticles on a carbon felt cathode in heterogeneous EF degradation of aspirin in wastewater. Taking advantage of the ferromagnetic properties of magnetite nanoparticles, we applied magnets to attract and hold the synthesized magnetite nanoparticles onto the cathode, resulting in improved immobilization and ultimately improved EF degradation of aspirin.

2. EXPERIMENTAL SECTION

2.1. Chemicals, Materials, and Characterization. All reagents used were of reagent grade and were used without

https://doi.org/10.1021/acsomega.2c00627
ACS Omega 2022, 7, 19261−19269

further purification. All solutions were made using high-purity water obtained from a Millipore Milli-Q system with resistivity >18 MΩ cm at room temperature (23 ± 2 °C). Iron(II) sulfate heptahydrate, aspirin, paracetamol, and ciprofloxacin were all purchased from Sigma Aldrich (South Africa). Sodium sulfate anhydrous was purchased from Rochelle Chemicals (South Africa), while ferric chloride hexahydrate ($FeCl_3{\cdot}6H_2O$) was obtained from Associated Chemical Enterprise. A carbon felt (from Carbone-Lorraine) and Ti_4O_7 (thin film deposited on Ti alloy from Saint-Gobain CREE) were purchased from France.

Fourier-transform infrared spectroscopy (FTIR) was conducted with a Bruker (South Africa) Alpha Sample Compartment RT-DLaTGS HR 0.8. UV−vis spectroscopic measurements were performed with a Cary 60 from Agilent Technologies. The crystallinity of the synthesized nanoparticles was determined using an X-ray diffractometer (Rigaku Ultima IV, Japan) using Cu Ka radiation (*k*1/4 0.15406) with K-beta filter at 30 mA and 40 kV. Surface morphological studies were carried out using a TESCAN Vega 3(Czech Republic) scanning electron microscope coupled with an energy-dispersive X-ray spectrometer.

2.2. Preparation of the Magnetite (Fe_3O_4) Nanoparticle. Magnetite was synthesized following the coprecipitation method described by Nidheesh and colleagues.[39] In brief, the coprecipitation method from the reaction of ferric/ferrous ions and OH^- anions in aqueous conditions was used. Molar ratios of Fe^{2+}/Fe^{3+} were varied in a total iron concentration of 0.075 M in 100 mL. Ferric and ferrous salts were dissolved separately in 50 mL volumes and stirred gently for 10 min to ensure maximum homogeneity. A brown solution was obtained with pH ≈ 2.0. To this solution was added between 8−10 mL of 8.0 M NaOH dropwise while stirring. The solution immediately turned black upon addition of the NaOH drop due to the formation of magnetite suspension. A pH of ≈ 13.45 was observed after complete addition of NaOH, confirming complete Fe_3O_4 formation. This was followed by dialysis in excess deionized water (dH_2O) using a dialysis tube to get rid of the counter ions. Filtration of the nanoparticle suspension was done, and the obtained crystals were oven-dried at 75 °C for 24 h, ground to powder using a mortar and pestle, and stored in a closed container ready for further applications. Magnetite (Fe_3O_4) was prepared from eight different Fe^{2+}/Fe^{3+} ratios, namely, 1:1, 1:2, 1:3, 1:4, 1:6, 2:1, 3:1, and 4:1 and tested in heterogeneous EF removal of aspirin in water.

2.3. Electro-Fenton Cell Setup and Degradation. The schematic of the setup is presented in Scheme 1. A 600 mL beaker was used as an undivided cell for all the reactions reported herein. The anode made of stoichiometric titanium oxide, that is, Ti_4O_7 coated on a 6 cm × 4 cm titanium metal, was placed at the center of the cell in all the reactions. The carbon felt cathode of 23 cm × 12 cm × 0.5 cm was placed right round the interior perimeter of the cell surrounding the anode at the center with an inter electrode distance of 1 cm. Rectangular magnet bars (5 cm × 2.2 cm × 0.8 cm) were connected touching each other (north pole to south pole) and fixed using rubber bands around the outside of the beaker to exert a magnetic attraction with magnetite nanoparticles immobilized on the CF cathode of dimensions 23 cm × 12 cm × 0.5 cm. An optimized potential difference of 8.0 V was applied in all reactions. The immobilization of the catalyst on the CF was as follows: The catalyst was dispersed in an aqueous solution and poured into the reaction vessel with stirring. Once the magnet was fitted, the dispersed catalyst nanoparticles were all attracted onto the CF as pulled by the magnet and thus evenly distributed on the surface of the CF cathode. The decrease in the absorbance of each of the pharmaceutical at their λ_{max} from UV spectroscopic measurements was used to calculate the percentage degradation.

2.4. Electro-Fenton Experiments. For all reactions, 250 mL of 10 mg/L aspirin solution was used with a supporting electrolyte of 0.05 M Na_2SO_4. Similarly, 15 mg/L of magnetite nanoparticle catalyst was used in all reactions. Hydrogen peroxide was electro-generated in situ from the reduction of O_2 at the cathode under an optimized acidic pH of 3.5. Availability of dissolved oxygen for this cause was ensured by pumping in air using an air sparging pump at a rate of 1 L per minute, starting 10 min before the beginning of the degradation process.

3. RESULTS AND DISCUSSION

3.1. Characterization Results. *3.1.1. FTIR Results.* The characteristic FTIR functional groups for magnetite (prepared from different Fe^{2+}/Fe^{3+} ratios) are observed in Figure 1a. Prominent peaks were produced by the Fe−O stretch at around 588 cm^{-1}, a shoulder peak that is more prominent at higher Fe^{2+} concentrations, giving an indication that ferrous

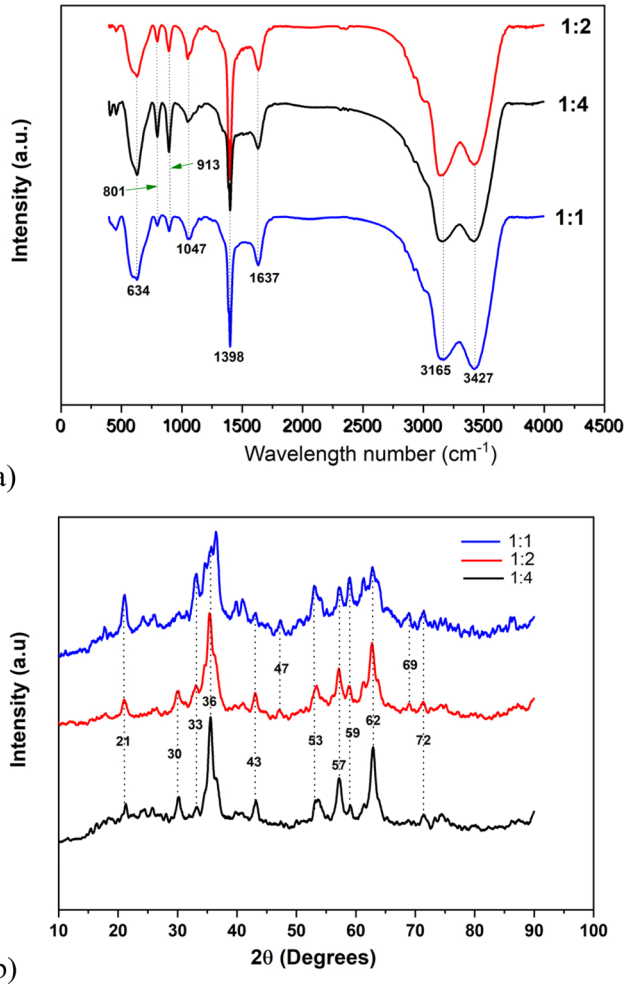

Figure 1. (a) FTIR and (b) XRD results for the magnetite nanoparticles synthesized with different Fe^{2+}/Fe^{3+} ratios of 1:1 (blue), 1:2 (red), and 1:4 (black).

https://doi.org/10.1021/acsomega.2c00627
ACS Omega 2022, 7, 19261−19269

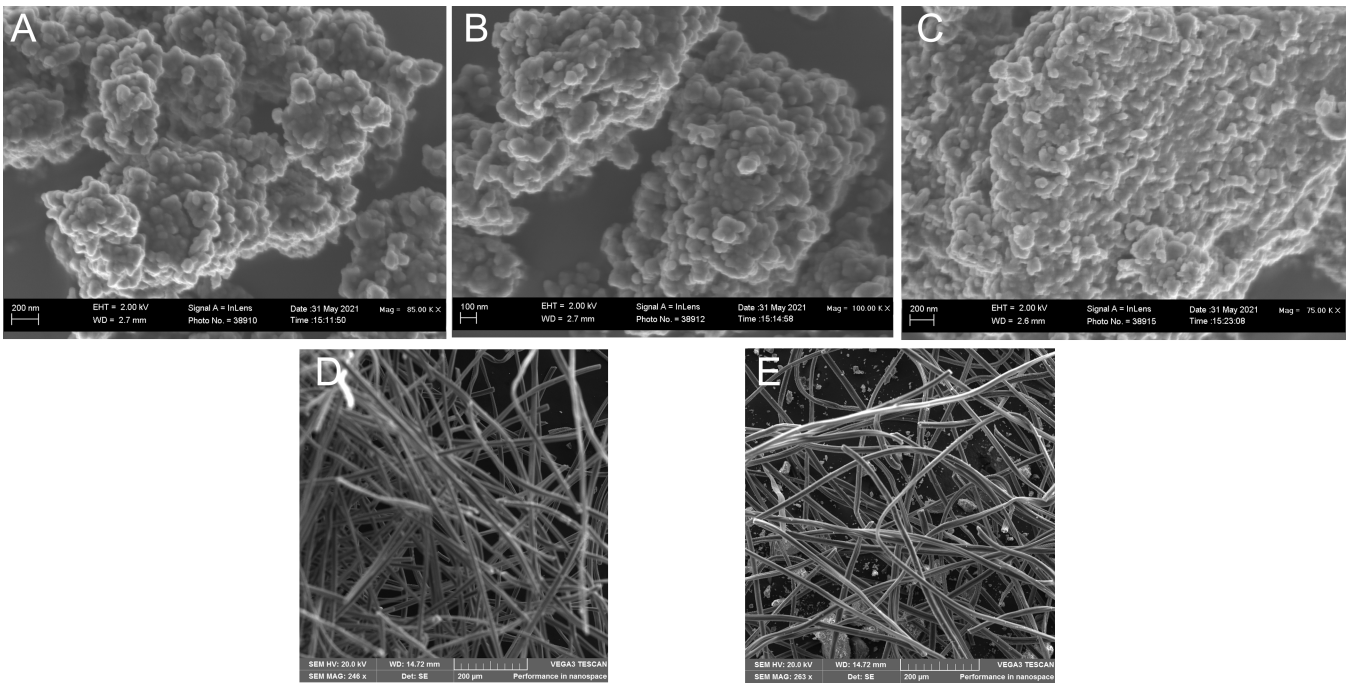

Figure 2. SEM images of magnetite nanoparticles (a−c) made from Fe^{2+}/Fe^{3+} = (a) (1:1), (b) (1:2), and (c) 1:4, (d) carbon felt (CF), and (e) magnetite-immobilized CF.

ions produce more stable Fe−O bonds in the lattice structure. In the same vein, Fe_3O_4 formation is confirmed by the peaks at 1631 and 588 cm^{-1}, both of which are prominent at higher Fe^{2+}/Fe^{3+} ratios, in agreement with the literature.[39] A prominent peak for the O−H is assigned to 3419 cm^{-1}, giving a clue of the presence of absorbed water by the nanoparticles.[39] The same authors suggested that the O−H peak may be due to the presence of iron hydroxyl functional groups in the form of $Fe(OH)_2$, $Fe(OH)_3$, or FeO(OH) formed during the dialysis stage of purifying the nanoparticles. The assumption for the presence of absorbed water is further supported by the peak at 1635 cm^{-1}, which can be assigned to the O−H stretches in water.[24] The FTIR spectra from the prepared magnetite of all Fe^{2+}/Fe^{3+} ratios are similar (Figure S1a,b).

3.1.2. XRD Analysis. The XRD 2θ characteristic peaks (Figure 1b) at 30.2, 35.5 (highest intensity), 43.2, 57.1, and 62.7° confirm the successful synthesis of magnetite nanoparticles for all the Fe^{2+}/Fe^{3+} ratios.[40,41] The ratio of Fe^{2+}/Fe^{3+} seems to affect the crystallinity of the magnetite. As seen in Figure 1b, the diffractogram of Fe^{2+}/Fe^{3+} 1:4 is more crystalline than that of Fe^{2+}/Fe^{3+} 1:1 owing to increase in the Fe^{3+} content. Nidheesh et al. reported that the crystalline nature of the synthesized magnetite nanoparticles increases with the increasing Fe^{3+} concentration.[39] There is a difference in the XRD spectra of the synthesized nanoparticles at peak 30.2° where the peak becomes more prominent with the increasing ferric ion concentration from 1:1, 1:2, to 1:4. The appearance of this peak at 30.2° is a suggestion for the presence of maghemite (γ−Fe_2O_3) in addition to magnetite nanoparticles. According to the literature, synthetic magnetite nanoparticles exist as a mixture of maghemite and magnetite if synthesized from Fe^{3+}/Fe^{2+} > 1.5 but exist in pure form at Fe^{3+}/Fe^{2+} < 1.5, with different magnetic properties.[42−44] This supposition is confirmed by the fact that pure maghemite has an XRD 2θ peak at ±30° according to the literature.[45,46] The XRD findings such suggest that the ratio of Fe^{2+}/Fe^{3+} affects the structural properties of magnetite.

3.1.3. SEM Analysis. The SEM images of magnetite synthesized from different ratios of Fe^{2+}/Fe^{3+} are presented in Figure 2a−c. Clusters of agglomerated nanoparticles are seen clearly. The SEM images of all the ratios are also similar. The CF shows well-distributed fibers intertwined leaving a dense network of pores of different sizes available for the nanoparticles to occupy. A comparison of Figure 2d (the CF network) and Figure 2e (CF and magnetite nanoparticle) shows successful immobilization of the magnetite nanoparticle within the network of the CF.

3.2. Electro-Fenton Degradation of Pharmaceuticals.

3.2.1. Fe^{2+}/Fe^{3+} Ratio Optimization in the Magnetite Catalyst. To investigate the optimal ratio of Fe^{2+}/Fe^{3+} for the degradation of aspirin in water by heterogeneous EF using magnetite nanoparticles, we probed magnetite nanoparticles synthesized from eight different ratios, namely, 1:1, 1:2, 1:3, 1:4, 1:6, 2:1, 3:1, and 4:1 with results presented in Figure 3a. Indeed, the theoretical ratio of Fe(II)/Fe(III) in magnetite is 1:2. However, some reports have shown that this ratio may vary owing to the aerobic aerial oxidation of surface Fe(II) to Fe(III), resulting in more Fe(III) ions at the expense of Fe(II) ions.[42,43] These variations in the ratio of Fe(II)/Fe(III) have been observed to affect (i) crystallization, (ii) saturation magnetization, and (iii) purity of magnetite. In a paper reported by Jiang and co-authors,[42] it is stated that at Fe(III)/Fe(II) > 1.5, there is a mixture of magnetite (Fe_3O_4) and maghemite (y-Fe_2O_3); and at Fe(III)/Fe(II) < 1.5, there is pure magnetite.

The effect of the Fe(II)/Fe(III) ratio on magnetite as shown by these authors[39,42−44] motivated us to investigate the catalytic performance of magnetite prepared from different ratios. Our hypothesis (that magnetite performance may vary from the synthetic composition of Fe(II)/Fe(III)) was supported by the observed variation in the catalytic response

https://doi.org/10.1021/acsomega.2c00627
ACS Omega 2022, 7, 19261−19269

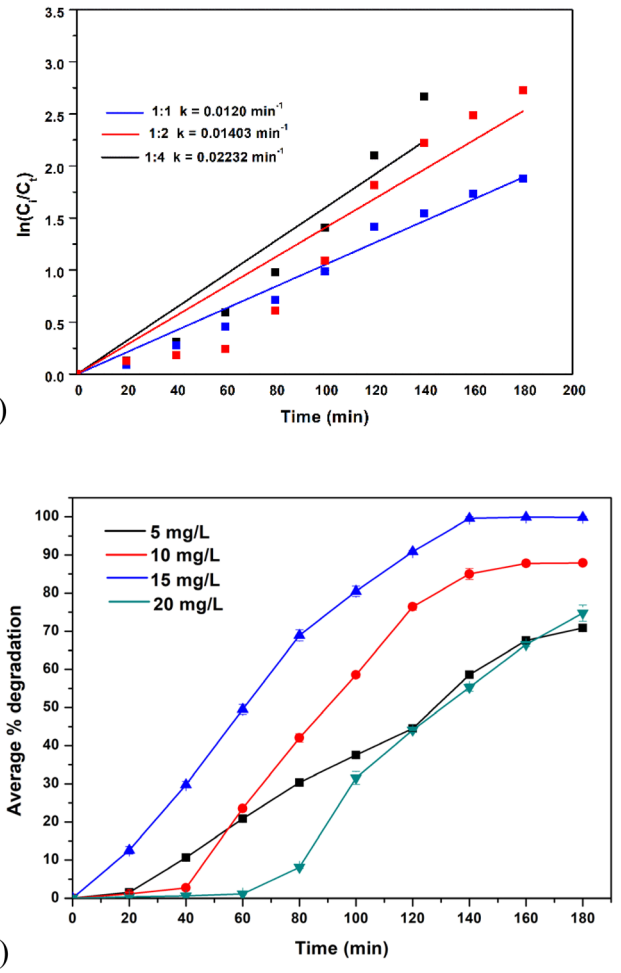

Figure 3. (a) Influence of different Fe^{2+}/Fe^{3+} ratios in the magnetite nanoparticle catalyst on the reaction rate constants in the heterogeneous EF. (b) Catalyst concentration optimization for magnetite-catalyzed EF removal of aspirin in water.

of the magnetites prepared from different Fe(II)/Fe(III) in our report (Figure 2). This variation supports some of the findings that the ratio of Fe(II)/Fe(III) in magnetite may deviate from the theoretical value of Fe(II)/Fe(III) 1:2. This also suggests that the properties of magnetite are influenced by the Fe(II)/Fe(III) ratio in synthesis.

Magnetite synthesized from the ratio of 1:4 (Fe^{2+}/Fe^{3+}) resulted in the highest hetero-EF catalytic degradation of aspirin. Complete degradation, i.e., 100% degradation, was achieved at this ratio after 140 min. An ideal Fenton catalyst is the one that provides and maintains appropriate amounts of both Fe^{2+} and Fe^{3+} ions throughout the reaction. Since magnetite synthesized with an Fe^{2+}/Fe^{3+} ratio of 1:4 in magnetite gave the best performance, we therefore suggest that it provides the best Fe^{2+}/Fe^{3+} amounts with the most suitable crystallization and magnetic properties required for maximum catalysis and interaction with magnets for optimum immobilization on the CF cathode. The interconversion of Fe^{2+}/Fe^{3+} and vice versa (shown in eqs 1 and 2) during the Fenton reaction plays a significant role in maintaining the optimum concentrations of these ions.

$$Fe^{2+} + H_2O_2 \rightarrow Fe^{3+} + \cdot OH + OH^- \quad (1)$$

$$Fe^{3+} + H_2O_2 \rightarrow Fe^{2+} + \cdot O_2H + H^+ \quad (2)$$

The optimum Fe^{2+}/Fe^{3+} ratio in magnetite however varies as a function of the specific analyte degraded and the reaction conditions employed. For example, Nidheesh et al.[39] reported the ratio of 2:1 as the best for the degradation of rhodamine dye, and Xu and Wang[34] utilized a 1:2 ratio for the removal of 4-chlorophenol in water, while Lei et al.[2] used a 1:1 ratio in the degradation of phenol.

3.2.2. Effects of Catalyst Concentration. Four different catalyst loading values of 5, 10, 15, and 20 mg/L of the 1:4 ratio were investigated, and 15 mg/L gave the best degradation performance. Thus, this concentration was used for further degradation (Figure 3b). Catalyst performance increased linearly with the catalytic concentration from 5 to 15 mg/L above which a decline in performance is observed. At a lower catalyst loading, there is not enough Fe^{2+} to catalyze the decomposition of H_2O_2 to generate sufficient radicals for the degradation of the aspirin analyte. On the other hand, the decline in catalytic performance at 20 mg/L catalyst concentration can be due to the increase in the rate of scavenger reactions that deplete the system of the much-needed hydroxyl radicals and the iron catalyst in the form of both ferric and ferrous ions. Reactions 3 and 4 are typical examples of these unwanted scavenger reactions. It is important to note that the immobilized catalyst concentration is too small and negligible to cause any significant passivation on the cathode's reduction power owing to the fact that CF has a large surface area.

$$Fe^{3+} + H_2O_2 \rightarrow FeOOH^{2+} + H^+ \quad (3)$$

$$Fe^{2+} + \cdot OH \rightarrow Fe^{3+} + OH^- \quad (4)$$

3.2.3. Effects of pH. One of the notable advantages of heterogeneous EF is in its flexibility to occur over a wider pH range unlike the homogeneous counterpart, which is limited to a narrow pH range between 2.5 and 3.0. This pH robustness extends the use of heterogeneous EF in real wastewater treatment applications. The effect of pH (2−12) on the EF degradation of aspirin was studied. More than 80% aspirin removal was recorded in all cases, proving that the reaction efficiency is less dependent on a specific pH as shown in Figure 4 (see more pH points in Figure S3). The highest removal efficiency occurred at pH 3.5, and this pH was thus chosen as the optimum pH for subsequent runs.

Initial pH is a very important parameter for the EF reaction, as it plays a crucial role in maintaining the Fe^{2+}/Fe^{3+} and H_2O_2 redox reactions by affecting the solubility of the iron oxide nanoparticles (leaching). Furthermore, pH studies have shown that catalyst leaching is high at acidic pHs, making the predominant mechanism more of homogeneous EF at pH < 4.5. The introduction of magnets to keep the immobilized nanoparticles on the CF is chiefly responsible for the good catalytic activity above pH 7 where the EF reaction overwhelmingly occurs via the heterogeneous mechanism on the surface of magnetite nanoparticles as alluded by Ganiyu and co-authors.[47] This is due to the large surface area retained by these nanoparticles as there is minimal catalyst leaching and falling off the CF into the solution where they are liable to agglomeration, consequently giving rise to poor catalytic activity. The exact surface reaction pathway at these high pHs has been a subject of intrinsic study thus far, with no definite consensus yet. However, most scholars agree that, like the homogeneous EF, the reaction fits into the Haber−Weiss circle mechanism. Furthermore, the proposed mechanism by

https://doi.org/10.1021/acsomega.2c00627
ACS Omega 2022, 7, 19261−19269

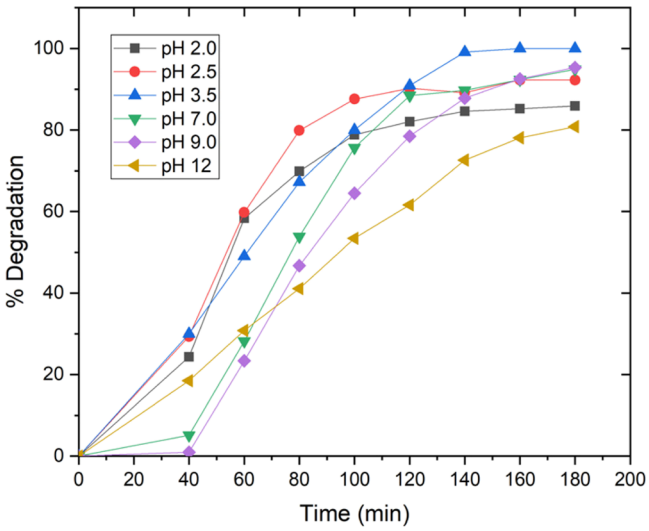

Figure 4. Percentage removal of aspirin by heterogeneous EF as a function of pH.

the same authors seems to satisfy our inquisition by best describing the phenomenon as represented by eqs 5−10.[47]

$$\equiv Fe^{3+} - OH + e^- \rightarrow \equiv Fe^{2+} - OH \quad (5)$$

$$\equiv Fe^{3+} - OH + H_2O_2 \leftrightarrow \equiv Fe^{3+} - OH\,(H_2O_2)_{(s)} \quad (6)$$

$$\equiv Fe^{3+} - OH\,(H_2O_2)_{(s)} \rightarrow \equiv Fe^{2+} - OH\,(HO\cdot_2)_{(s)} + H^+ \quad (7)$$

$$\equiv Fe^{2+} - OH\,(HO\cdot_2)_{(s)} \rightarrow \equiv Fe^{2+} - OH + HO\cdot_2 + H^+ \quad (8)$$

$$\equiv Fe^{2+} - OH + H_2O_2 \rightarrow \equiv Fe^{3+} - OH + \cdot OH + OH^- \quad (9)$$

$$\cdot OH + \text{Organic pollutants} \rightarrow \text{byproducts} \rightarrow CO_2 + H_2O \quad (10)$$

$$\cdot OH + H_2O_2 \rightarrow HO\cdot_2 + H_2O \quad (11)$$

It is important to note that pH does not remain constant during the degradation due to the rate of reaction fluctuations between the anodic oxidation (which tends to lower pH by production of H^+ through water oxidation) and the Fenton reaction producing a hydroxyl anion, which sequentially mops away the H^+ to form water, thereby countering the anodic effect.

$$H_2O \rightarrow \cdot OH + H^+ + e^- \text{ (Anodic oxidation)} \quad (12)$$

$$Fe^{3+} + e^- \rightarrow Fe^{2+} \text{ (Cathodic reaction)} \quad (13)$$

$$Fe^{2+} + H_2O_2 \rightarrow Fe^{3+} + \cdot OH + OH^- \text{ (Fenton reaction)} \quad (14)$$

In addition, it has been observed that there is a formation of carboxylic acid intermediates, which also contribute to moving the initial pH toward acidity.

3.2.4. Voltage/Current Effect. An applied potential difference of 8.0 V was the optimal voltage for the heterogeneous EF degradation of aspirin in wastewater using a magnetite nanoparticle catalyst (Figure 5a). Voltage plays a pivotal role in EF, and hence, an optimal voltage is maintained to maximize

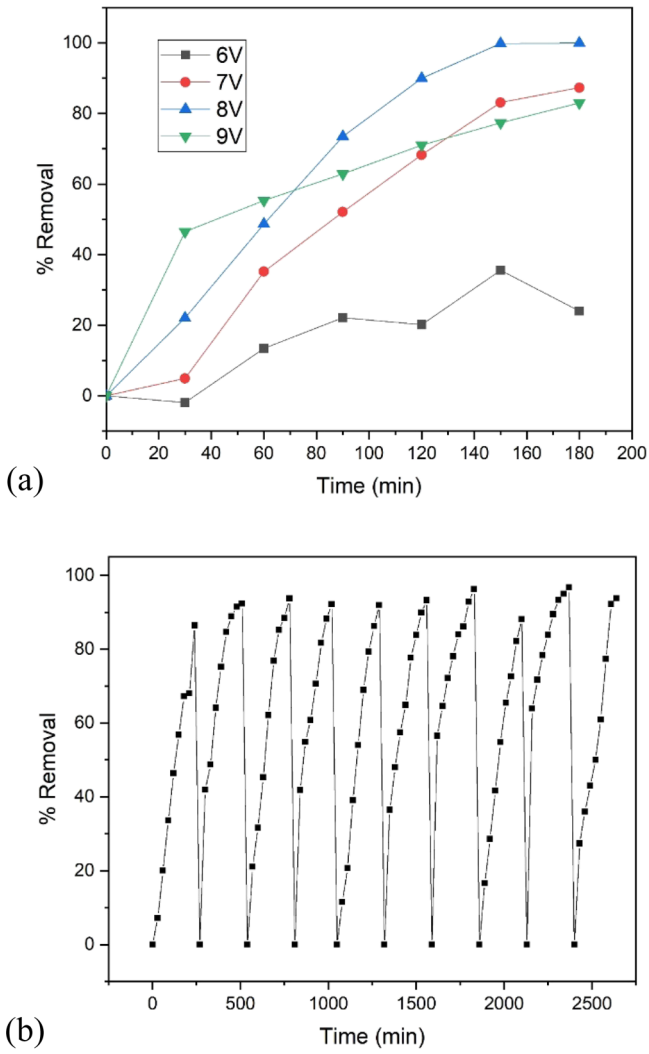

Figure 5. (a) Effect of voltage on the EF degradation of aspirin. (b) Effectiveness of magnetite nanoparticle catalyst reusability in EF removal of aspirin after 10 consecutive (cycles) for 2400 min (10 runs, 4 h each run).

the degradation of the target water contaminant at the lowest possible energy consumption. There is a linear increase in catalytic activity with increasing voltage from 6 to 8 V due to the promotion of EF in three main ways. First, the electro-regeneration of the Fe^{2+} catalyst from the cathodic reduction of Fe^{3+} is actively increased at high voltage, thereby increasing the rate of reaction. Second, anodic oxidation of water responds positively with the increasing voltage, creating a synergy with the improved catalyst regeneration at the cathode that amplifies EF degradation of organic pollutants in water. Third, the in situ electro-generation of H_2O_2 by the cathodic reduction of oxygen is proportionately dependent on the applied voltage.

However, as voltage is increased further above the optimum (above 8 V), an increase in scavenging side reactions is expected, thereby lowering the degradation of organic contaminants by EF by reducing effective production of hydroxyl radicals through the poisoning of the catalyst. In addition, it is noted that at high voltages, there is increased decomposition of H_2O_2 and the evolution of H_2 gas at the cathode. In addition, magnetite catalyst leaching is also exacerbated at high voltages above 8.0 V, leading to reduced

https://doi.org/10.1021/acsomega.2c00627
ACS Omega 2022, 7, 19261−19269

catalytic activity. Of note, the highest initial rate of reaction (the first 30 min) is at 9 V, which slumped thereafter. The sudden initial rise in EF activity at 9 V is accredited to a boost in the anodic reaction, hydrogen peroxide electro-generation, and Fe^{2+} catalyst electro-regeneration from the reduction of Fe^{3+} due to the applied high voltage. The observed subsequent slump in activity is owing to the significant increase in scavenging reactions as discussed previously.

3.2.5. Catalyst Reusability Test. The stability of a catalyst is an important parameter in catalysis because it suggests the reusability of a catalyst over many cycles without loss of activity. Both physical and chemical deformations are possible on a catalyst during a reaction, which ultimately lead to the catalyst's loss of stability and activity. For example, chemical fouling leads to the gradual passivation of the catalyst by forming a thin unreactive layer, e.g., a metal oxide via oxidation, on the surface of a metal catalyst, thereby rendering it less active. Figure 5b shows the application of the magnetite as a heterogeneous EF catalyst over 10 cycles. The magnetite nanoparticles show good resilience to deformation under both chemical and physical stress as an EF catalyst as shown by the percentage removal of aspirin that ranges from 86.4 to 97.7%. The stability of the magnetite can be ascribed to two factors. First, there is reduced leaching in this EF reaction at pH 3.5 used instead of the traditionally used pH 3.0 in the literature.[30,34] Leaching is known to increase with the increasing acidity, and it remains one of the unresolved challenges confronting heterogeneous EF. Second, the stability exhibited by the magnetite nanoparticles in catalyzing EF degradation of aspirin is due to minimal agglomeration resulting from the magnetic immobilization approach.

3.2.6. Radical Trapping Effect. To show the predominant role of hydroxyl radicals in this heterogeneous EF system, trapping experiments using isopropanol were carried out. Figure 6a shows the inhibition role played by isopropanol in the EF degradation of aspirin. A very significant percentage degradation difference of 77.8% between the uninhibited (positive control) and the inhibited (negative control (with isopropanol)) is a clear demonstration that the EF reaction is a radical-driven reaction directly fueled by the hydroxyl radicals. The low degradation that still occurred in the presence of the radical scavenging isopropanol can be because of the effect of other less-significant radicals and the effect of the anodic oxidation of aspirin.

3.2.7. Effect of Analyte Variation. To investigate the robustness of the reported approach, we undertook to degrade acetaminophen (commonly known as paracetamol) and an antibiotic, ciprofloxacin, in addition to aspirin. As seen from Figure 6b, high percentage degradations of 94.3% (aspirin), 88% (ciprofloxacin), and 80% (paracetamol) in 3 h were obtained for all three different pharmaceuticals chosen. This shows the effectiveness of the improvement strategy reported toward other pharmaceutical in a mixture.

3.2.8. Effects of Magnet Bars on Magnetite Immobilization. To demonstrate the advantages of magnet bars in enhancing magnetite immobilization on the CF and hence the overall heterogeneous EF degradation of aspirin, we set a negative control (reaction without magnet bars) versus a positive control (one with magnet bars). The differences in the rate of reaction and overall percentage aspirin degradation between the two is a measure of the effectiveness of magnets in this reaction. From Figure 6c, the initial rate of reaction is seen to be the same for the first 30 min after which the reaction

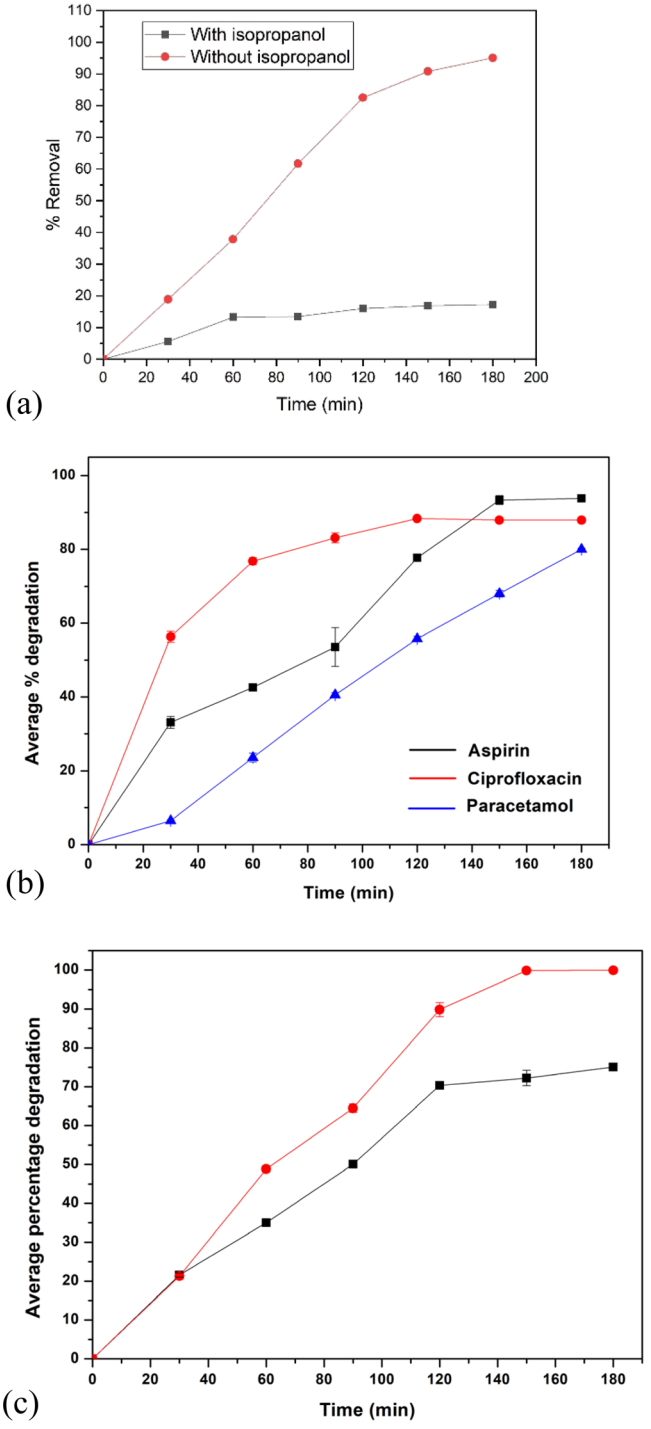

Figure 6. (a) Effects of the use of isopropanol hydroxyl radical trap on the EF degradation of aspirin. (b) Effect of pharmaceutical (analyte) variation on the effectiveness of heterogeneous EF using magnetite. (c) Effect of magnetic bars in enhancing the immobilization of magnetite nanoparticles on the CF cathode.

without magnets shows less activity. This observation can be explained in terms of the leaching of the immobilized magnetite nanoparticles from the CF support. Once leached, these nanoparticles have high susceptibility to aggregate, forming agglomerated clusters with less surface area as previously explained. Furthermore, leached magnetite nanoparticles may lead to a slower EF reaction, since they take time to reach the cathode for surface ferric ions to be reduced to the

https://doi.org/10.1021/acsomega.2c00627
ACS Omega 2022, 7, 19261−19269

active ferrous ions by mass transfer. On the contrary, cathode-immobilized nanoparticles are in direct contact with the cathode and therefore are easily liable to redox reactions needed for heterogeneous EF degradation of organics. The use of magnet bars thus enhanced the heterogeneous EF process.

4. CONCLUSIONS

A simple novel approach to the heterogeneous EF process using magnetite nanoparticles immobilized on a CF cathode with the aid of magnets has been successfully demonstrated. High aspirin percentage removal or degradation up to 100% was achieved under optimized conditions of pH 3.5 using 15 mg/L of the magnetite nanoparticles synthesized from an Fe^{2+}/Fe^{3+} ratio of 1:4. Three different pharmaceuticals, namely, aspirin, paracetamol, and ciprofloxacin, were degraded in wastewater, suggesting the robustness of the approach. The challenge of narrow pH usually experienced in homogeneous EF was mitigated in this study as shown by the degradation of aspirin over a wider pH range ranging from 2.0 to 12.0. Good catalyst reusability was confirmed by using the same catalyst for 10 cycles, proving an enhanced degree of magnetite catalyst stability under the influence of magnetic immobilization on the CF. This method reported thus contributes another effective way of improving heterogeneous EF wastewater treatment.

■ ASSOCIATED CONTENT

Supporting Information

The Supporting Information is available free of charge at https://pubs.acs.org/doi/10.1021/acsomega.2c00627.

(Figure S1) FTIR results for the synthesized magnetite nanoparticles of all the Fe^{2+}/Fe^{3+} ratios; (Figure S2) effects of different Fe^{2+}/Fe^{3+} ratios in the catalytic performance of magnetite nanoparticles toward the HEF degradation of aspirin; and (Figure S3) pH effect on the magnetite catalyst EF degradation of aspirin in wastewater (PDF)

■ AUTHOR INFORMATION

Corresponding Author

Omotayo A. Arotiba − *Department of Chemical Sciences and Centre for Nanomaterials Science Research, University of Johannesburg, Johannesburg 2028, South Africa;* orcid.org/0000-0002-8227-8684; Email: oarotiba@uj.ac.za

Author

Charles Muzenda − *Department of Chemical Sciences, University of Johannesburg, Johannesburg 2028, South Africa*

Complete contact information is available at: https://pubs.acs.org/10.1021/acsomega.2c00627

Notes

The authors declare no competing financial interest.

■ ACKNOWLEDGMENTS

We gratefully acknowledge financial support from the National Research Foundation, South Africa (CPRR grant number 118546). The assistance provided by Ms. Nelile Ndzinisa and Ms. Elelwani Ramudzwagi during their work integrated learning program at the electrochemistry research group is appreciated.

■ REFERENCES

(1) Munoz, M.; de Pedro, Z. M.; Casas, J. A.; Rodriguez, J. J. Preparation of Magnetite-Based Catalysts and Their Application in Heterogeneous Fenton Oxidation - A Review. *Appl. Catal. B Environ.* **2015**, *176*−*177*, 249−265.

(2) Lei, Y.; Chen, C.; Tu, Y.; Huang, Y.; Zhang, H. Heterogeneous degradation of organic pollutants by persulfate activated by CuO-Fe_3O_4: mechanism, stability, and effects of pH and bicarbonate ions. *Environ. Sci. Technol.* **2015**, *49*, 6838−6845.

(3) Meijide, J.; Pazos, M.; Sanromán, M. Á. Heterogeneous Electro-Fenton Catalyst for 1-Butylpyridinium Chloride Degradation. *Environ. Sci. Pollut. Res.* **2019**, *26*, 3145−3156.

(4) Poza-Nogueiras, V.; Rosales, E.; Pazos, M.; Sanromán, M. Á. Current Advances and Trends in Electro-Fenton Process Using Heterogeneous Catalysts − A Review. *Chemosphere* **2018**, *201*, 399−416.

(5) Bouzayani, B.; Meijide, J.; Pazos, M.; Elaoud, S. C.; Sanroman, M. A. Removal of Polyvinylamine Sulfonate Anthrapyridone Dye by Application of Heterogeneous Electro-Fenton Process. *Environ. Sci. Pollut. Res.* **2017**, *24*, 18309−18319.

(6) Zhang, C.; Zhou, M.; Ren, G.; Yu, X.; Ma, L.; Yang, J.; Yu, F. Heterogeneous electro-Fenton using modified iron-carbon as catalyst for 2,4-dichlorophenol degradation: influence factors, mechanism and degradation pathway. *Water Res.* **2015**, *70*, 414−424.

(7) Phong Vo, H. N.; Le, G. K.; Hong Nguyen, T. M.; Bui, X. T.; Nguyen, K. H.; Rene, E. R.; Vo, T. D. H.; Thanh Cao, N. D.; Mohan, R. Acetaminophen Micropollutant: Historical and Current Occurrences, Toxicity, Removal Strategies and Transformation Pathways in Different Environments. *Chemosphere* **2019**, *236*, No. 124391.

(8) Bilal, M.; Ashraf, S. S.; Barceló, D.; Iqbal, H. M. N. Biocatalytic Degradation/Redefining "Removal" Fate of Pharmaceutically Active Compounds and Antibiotics in the Aquatic Environment. *Sci. Total Environ.* **2019**, *691*, 1190−1211.

(9) Svendsen, S. B.; El-taliawy, H.; Carvalho, P. N.; Bester, K. Concentration Dependent Degradation of Pharmaceuticals in WWTP Effluent by Biofilm Reactors. *Water Res.* **2020**, *186*, No. 116389.

(10) Girija Shankar, E.; Aishwarya, M.; Khan, A.; Kumar, A. B. V. K.; Yu, J. S. Efficient Solar Light Photocatalytic Degradation of Commercial Pharmaceutical Drug and Dye Using RGO-PANI Assisted c-ZnO Heterojunction Nanocomposites. *Ceram. Int.* **2021**, *47*, 23770−23780.

(11) Wang, D.; Zhang, H.; Yu, Y.; Zhang, J. Enhanced Abatement of Pharmaceuticals by Permanganate via the Addition of Co_3O_4 Nanoparticles. *Chemosphere* **2021**, *282*, No. 131115.

(12) Dang, V. D.; Adorna, J.; Annadurai, T.; Bui, T. A. N.; Tran, H. L.; Lin, L. Y.; Doong, R. A. Indirect Z-Scheme Nitrogen-Doped Carbon Dot Decorated Bi_2MoO_6/g-C_3N_4 Photocatalyst for Enhanced Visible-Light-Driven Degradation of Ciprofloxacin. *Chem. Eng. J.* **2021**, *422*, No. 130103.

(13) Konstas, P. S.; Kosma, C.; Konstantinou, I.; Albanis, T. Photocatalytic Treatment of Pharmaceuticals in Real Hospital Wastewaters for Effluent Quality Amelioration. *Water* **2019**, *11*, 2165.

(14) Ngumba, E.; Gachanja, A.; Tuhkanen, T. Removal of Selected Antibiotics and Antiretroviral Drugs during Post-Treatment of Municipal Wastewater with UV, UV/Chlorine and UV/Hydrogen Peroxide. *Water Environ. J.* **2020**, *34*, 692−703.

(15) Martínez-Pachón, D.; Echeverry-Gallego, R. A.; Serna-Galvis, E. A.; Villarreal, J. M.; Botero-Coy, A. M.; Hernández, F.; Torres-Palma, R. A.; Moncayo-Lasso, A. Treatment of Wastewater Effluents from Bogotá − Colombia by the Photo-Electro-Fenton Process: Elimination of Bacteria and Pharmaceutical. *Sci. Total Environ.* **2021**, *772*, No. 144890.

(16) Emeji, I. C.; Ama, O. M.; Khoele, K.; Osifo, P. O.; Ray, S. S. Electro-Fenton Degradation of Selected Antiretroviral Drugs Using a Low-Cost Iron-Modified Carbon-Cloth Electrode. *Electrocatalysis* **2021**, *12*, 327−339.

(17) Zhao, H.; Qian, L.; Chen, Y.; Wang, Q.; Zhao, G. Selective Catalytic Two-Electron O_2 Reduction for Onsite Efficient Oxidation

Reaction in Heterogeneous Electro-Fenton Process. *Chem. Eng. J.* **2018**, *332*, 486−498.
(18) Wang, A.; Zhang, Y.; Han, S.; Guo, C.; Wen, Z.; Tian, X.; Li, J. Electro-Fenton oxidation of a β-lactam antibiotic cefoperazone: Mineralization, biodegradability and degradation mechanism. *Chemosphere* **2021**, *270*, No. 129486.
(19) Wang, W.; Li, Y.; Li, Y.; Zhou, M.; Arotiba, O. A. Electro-Fenton and Photoelectro-Fenton Degradation of Sulfamethazine Using an Active Gas Diffusion Electrode without Aeration. *Chemosphere* **2020**, *250*, No. 126177.
(20) Sirés, I.; Brillas, E. Upgrading and Expanding the Electro-Fenton and Related Processes. *Curr. Opin. Electrochem.* **2021**, *27*, No. 100686.
(21) Orimolade, B. O.; Zwane, B. N.; Koiki, B. A.; Rivallin, M.; Bechelany, M.; Mabuba, N.; Lesage, G.; Cretin, M.; Arotiba, O. A. Coupling Cathodic Electro-Fenton with Anodic Photo-Electrochemical Oxidation: A Feasibility Study on the Mineralization of Paracetamol. *J. Environ. Chem. Eng.* **2020**, *8*, No. 104394.
(22) Zwane, B. N.; Orimolade, B. O.; Koiki, B. A.; Mabuba, N.; Gomri, C.; Petit, E.; Bonniol, V.; Lesage, G.; Rivallin, M.; Cretin, M.; et al. Combined Electro-Fenton and Anodic Oxidation Processes at a Sub-Stoichiometric Titanium Oxide (Ti_4O_7) Ceramic Electrode for the Degradation of Tetracycline in Water. *Water* **2021**, *13*, 2772.
(23) Dhakshinamoorthy, A.; Navalon, S.; Alvaro, M. Metal Nanoparticles as Heterogeneous Fenton Catalysts. *ChemSusChem* **2012**, *5*, 46−64.
(24) Es'haghzade, Z.; Pajootan, E.; Bahrami, H.; Arami, M. Facile Synthesis of Fe_3O_4 Nanoparticles via Aqueous Based Electro Chemical Route for Heterogeneous Electro-Fenton Removal of Azo Dyes. *J. Taiwan Inst. Chem. Eng.* **2017**, *71*, 91−105.
(25) Ganiyu, S. O.; Le, T. X. H.; Bechelany, M.; Esposito, G.; van Hullebusch, E. D.; Oturan, M. A.; Cretin, M. A hierarchical CoFe-layered double hydroxide modified carbon-felt cathode for heterogeneous electro-Fenton process. *J. Mater. Chem. A* **2017**, *5*, 3655−3666.
(26) Zhou, L.; Zhou, M.; Hu, Z.; Bi, Z.; Serrano, K. G. Chemically Modified Graphite Felt as an Efficient Cathode in Electro-Fenton for p-Nitrophenol Degradation. *Electrochim. Acta* **2014**, *140*, 376−383.
(27) Peng, Q.; Zhao, H.; Qian, L.; Wang, Y.; Zhao, G. Design of a Neutral Photo-Electro-Fenton System with 3D-Ordered Macroporous Fe_2O_3/Carbon Aerogel Cathode: High Activity and Low Energy Consumption. *Appl. Catal. B Environ.* **2015**, *174*, 157−166.
(28) Wang, Y.; Liu, Y.; Li, X.; Zeng, F.; Liu, H. A Highly-Ordered Porous Carbon Material Based Cathode for Energy-Efficient Electro-Fenton Process. *Sep. Purif. Technol.* **2013**, *106*, 32−37.
(29) Peleyeju, M. G.; Arotiba, O. A. Recent Trend in Visible-Light Photoelectrocatalytic Systems for Degradation of Organic Contaminants in Water/Wastewater. *Environ. Sci. Water Res. Technol.* **2018**, *4*, 1389−1411.
(30) Babuponnusami, A.; Muthukumar, K. A Review on Fenton and Improvements to the Fenton Process for Wastewater Treatment. *J. Environ. Chem. Eng.* **2014**, *2*, 557−572.
(31) Iglesias, O.; Meijide, J.; Bocos, E.; Sanromán, M. Á.; Pazos, M. New Approaches on Heterogeneous Electro-Fenton Treatment of Winery Wastewater. *Electrochim. Acta* **2015**, *169*, 134−141.
(32) Yu, F.; Wang, Y.; Ma, H.; Zhou, M. Hydrothermal Synthesis of FeS2 as a Highly Efficient Heterogeneous Electro-Fenton Catalyst to Degrade Diclofenac via Molecular Oxygen Effects for Fe(II)/Fe(III) Cycle. *Sep. Purif. Technol.* **2020**, *248*, No. 117022.
(33) Tian, Y.; Zhou, M.; Pan, Y.; Du, X.; Wang, Q. MoS_2 as Highly Efficient Co-Catalyst Enhancing the Performance of Fe^0 Based Electro-Fenton Process in Degradation of Sulfamethazine: Approach and Mechanism. *Chem. Eng. J.* **2021**, *403*, No. 126361.
(34) Xu, L.; Wang, J. Magnetic Nanoscaled Fe_3O_4/CeO_2 Composite as an Efficient Fenton-Like Heterogeneous Catalyst for Degradation of 4- Chlorophenol. *Environ. Sci. Technol.* **2012**, *46*, 10145−10153.
(35) Pereira, M. C.; Oliveira, L. C. A.; Murad, E. Iron Oxide Catalysts: Fenton and Fentonlike Reactions − a Review. *Clay Miner.* **2012**, *47*, 285−302.
(36) Divyapriya, G.; Nambi, I. M.; Senthilnathan, J. Nanocatalysts in Fenton Based Advanced Oxidation Process for Water and Wastewater Treatment. *Bionanosci. J.* **2016**, *10*, 356.
(37) Zhao, W. G. Catalytic Activity of MOF (2Fe/Co)/Carbon Aerogel for Improving H_2O_2 and ·OH Generation in Solar Photo − Electro − Fenton Process. *Appl. Catal. B: Environ.* **2017**, *203*, 127−137.
(38) Hammouda, S.; Fourcade, F.; Assadi, A.; Soutrel, I.; Amrane, A.; Monser, L. Effective Heterogeneous Electro-Fenton Process for the Degradation of a Malodorous Compound, Indole Using Iron Loaded Alginate Beads as a Reusable Catalyst. *Appl. Catal. B: Environ.* **2016**, *182*, 47−58.
(39) Nidheesh, P. V.; Gandhimathi, R.; Velmathi, S.; Sanjini, N. S. Magnetite as a Heterogeneous Electro Fenton Catalyst for the Removal of Rhodamine B from Aqueous Solution. *RSC Adv.* **2014**, *4*, 5698−5708.
(40) Wang, Y.; Zhao, H.; Zhao, G. Highly Ordered Mesoporous Fe_3O_4@Carbon Embedded Composite: High Catalytic Activity, Wide pH Range and Stability for Heterogeneous Electro-Fenton. *Electroanalysis* **2016**, *28*, 169−176.
(41) Sun, S.; Zeng, H. Size-Controlled Synthesis of Magnetite Nanoparticles. *J. Am. Chem. Soc.* **2002**, *124*, 8204−8205.
(42) Jiang, W.; Lai, K. L.; Hu, H.; Zeng, X. B.; Lan, F.; Liu, K. X.; Wu, Y.; Gu, Z. W. The Effect of [Fe3+]/[Fe2+] Molar Ratio and Iron Salts Concentration on the Properties of Superparamagnetic Iron Oxide Nanoparticles in the Water/Ethanol/Toluene System. *J. Nanopart. Res.* **2011**, *13*, 5135−5145.
(43) Maity, D.; Agrawal, D. C. Synthesis of Iron Oxide Nanoparticles under Oxidizing Environment and Their Stabilization in Aqueous and Non-Aqueous Media. *J. Magn. Magn. Mater.* **2007**, *308*, 46−55.
(44) Iida, H.; Takayanagi, K.; Nakanishi, T.; Osaka, T. Synthesis of Fe_3O_4 Nanoparticles with Various Sizes and Magnetic Properties by Controlled Hydrolysis. *J. Colloid Interface Sci.* **2007**, *314*, 274−280.
(45) Tuutijärvi, T.; Lu, J.; Sillanpä, M.; Chen, G. As(V) Adsorption on Maghemite Nanoparticles. *J. Hazard. Mater.* **2009**, *166*, 1415−1420.
(46) Lee, S. J.; Jeong, J. R.; Shin, S. C.; Kim, J. C.; Kim, J. D. Synthesis and Characterization of Superparamagnetic Maghemite Nanoparticles Prepared by Coprecipitation Technique. *J. Magn. Magn. Mater.* **2004**, *282*, 147−150.
(47) Ganiyu, S. O.; Zhou, M.; Martínez-huitle, C. A. Heterogeneous EF and photo EF processes: A critical review of fundamental principles and application for water/wastewater treatment. *Appl. Catal. B: Environ.* **2018**, *235*, 103−129.

https://doi.org/10.1021/acsomega.2c00627
ACS Omega 2022, 7, 19261−19269